Volume 24, No 2 | International Journal of Radiation Research, April 2026

Evaluation of distance and angular dependence of polycrystalline semiconductor dosimeters for Ir-192 brachytherapy source using experimental measurements and Monte Carlo simulations

M.J. Han[1#], S.W. Kang[1#], K.Y. Eom[1], I.A. Kim[1], J.S. Kim[1], B. Lee[2], W. Cho[3], J.B. Chung[1*]

[1]*Department of Radiation Oncology, Seoul National University Bundang Hospital, Seongnam 13620, Republic of Korea*
[2]*Department of Radiation Oncology, Inha University Hospital, Incheon 22332, Republic of Korea*
[3]*Department of Radiation Oncology, Seoul National University Boramae Medical Center, Seoul 07061, Republic of Korea*

► ***Original article***

Corresponding author:
Jin-Beom Chung, Ph. D.,
E-mail:
jbchung1213@gmail.com

Received: March 2025
Final revised: September 2025
Accepted: November 2025

Int. J. Radiat. Res., April 2026; 24(2): 317-322

DOI: 10.61186/ijrr.24.2.3

Keywords: *Dosimeters, semiconductors, brachytherapy, iridium-192 radioisotope, Monte Carlo simulation, quality assurance.*

ABSTRACT

Background: This study evaluates the distance and angular dependence of polycrystalline semiconductor-based dosimeters (PSDs) using lead (II) iodide (PbI_2) (PbI_2 PSD) and lead (II) oxide (PbO) (PbO PSD) for Ir-192 brachytherapy source. Experimental measurements were compared with Monte Carlo (MC) simulations to verify the dosimeters' performance and accuracy. ***Materials and Methods:*** PSDs were fabricated using PbI_2 and PbO as photoconductive materials, with a thin-film deposition process ensuring uniformity. Distance dependence was assessed by measuring dosimeter responses at source-to-surface distances ranging from 1 cm to 8 cm at 0.25 cm intervals, while angular dependence was evaluated at angles from 0° to 60° in 15° increments. MC simulations using the Geant4 Application for Tomographic Emission (GATE) v9.1 were conducted under identical conditions to validate the experimental measurements. ***Results:*** The experimental and simulated data demonstrated a strong agreement with the inverse-square law, with determination coefficient (R^2) exceeding 0.98 for PbI_2 and PbO PSDs. The distance at which the signal intensity dropped by 50% (D_{50}) for measurements and simulations was 1.493 cm and 1.487 cm for PbI_2 PSD, respectively, and 1.488 cm and 1.481 cm for PbO PSD. Angular dependence analysis showed a decrease in response with increasing angle, with PbO PSD exhibiting slightly larger discrepancies (maximum difference of 5.48%) compared to PbI_2 PSD (maximum difference of 4.56%) between measurements and simulations. ***Conclusion:*** PbI_2 and PbO PSDs demonstrated predictable distance and angular dependence, closely aligning with MC simulations. However, angular correction factors may be necessary to improve dosimetric accuracy in clinical applications.

INTRODUCTION

High-dose-rate brachytherapy (HDR-BT) using Iridium-192 (Ir-192) radioisotopes is widely utilized to treat cancers, especially prostate, cervical, and breast cancers [1]. Accurate dose distribution measurement is crucial for enhancing treatment accuracy and necessitates the development of various dosimeters [2, 3]. Dose estimations by conventional dosimeters such as ionization chambers, thermos-luminescent dosimeters, and Gafchromic films are generally more accurate than those estimated using Monte Carlo (MC) simulations. However, conventional dosimeters may have limitations in specific clinical environments [3, 4].

Polycrystalline semiconductor-based dosimeters (PSDs) have recently gained attention due to their high sensitivity, reliability, compact size, high spatial resolution, and immunity to electromagnetic interference [5, 6]. Evaluating the stability of dose measurements in high-energy gamma-ray environments, such as those involving Ir-192 sources, is essential for their clinical application. This necessitates the analysis of distance and angular dependence to improve the accuracy of treatment planning [7, 8]. Mowlavi *et al.* [9] used the MCNP4C [10] code to calculate the relative dose, anisotropy dose function, and radial dose function TG-43 dosimetry parameters for a microselectron HDR Ir-192 source in a water phantom and compared them with the dose measured using Gafchromic RTQA film. However, research on the fabrication of PSDs using PbI_2 and PbO and evaluation of their distance and angle dependencies for Ir-192 radiation sources through measurements and MC simulations is limited.

This study aimed to evaluate the distance and angular dependence of the PSDs fabricated using lead

[DOI: 10.61186/ijrr.24.2.3]

(II) iodide (PbI_2) (PbI_2 PSD) and lead (II) oxide (PbO) (PbO PSD) for HDR Ir-192 sources by comparing the experimental measurements with the values obtained using Monte Carlo simulations. The PbI_2 and PbO PSDs were compared and assessed for their reliability for HDR-BT applications. To the best of our knowledge, this is the first study to systematically compare the performances of PbI_2 and PbO PSDs for an Ir-192 irradiation source by integrating experimental measurements and MC simulations. This dual approach enabled more robust validation of dosimetric performance than previous approaches that relied solely on measurements. Our results will facilitate the development of clinically applicable correction strategies by quantifying the distance and angular dependencies. This will advance the utility of PSDs in patient-specific quality assurance for HDR-BT.

MATERIALS AND METHODS

Fabrication of polycrystalline semiconductor-based dosimeter

Two types of PSDs were fabricated using PbI_2 (Sigma Aldrich, USA) and PbO (Sigma Aldrich, USA), respectively. Figure 1 shows their fabrication process. The lower electrode was composed of indium tin oxide glass (Moduscience, Korea) and ultrasonically cleaned for 30 min. The photoconductive material was mixed in powder form with a binder (polyvinyl butyral, Sigma Aldrich, USA) in a 3:1 ratio. The mixture was uniformly dispersed using a three-roll mill (EXAKT, Germany). A 150-μm-thick thin film was subsequently formed within a 1 × 1 cm mask frame via screen-printing deposition. The photoconductive material was placed on a granite surface plate for 30 min to improve the surface properties and minimize defects (surface roughness error within 5%). It was subsequently annealed at 70°C for 8 h. The upper electrode (Au wire, Sigma-Aldrich, USA; purity: 99.999%) was deposited via physical vapor deposition and had dimensions of 0.8 × 0.8 cm. The PSD was sealed to protect it from environmental factors such as humidity and temperature changes.

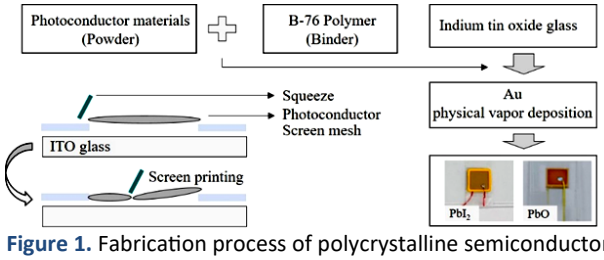

Figure 1. Fabrication process of polycrystalline semiconductor dosimeter using PbI2 and PbO materials.

Measurement of distance and angular dependence

Figure 2 shows the measurement setups for evaluating the distance and angular dependence of the PbI_2 and PbO PSDs. Table 1 summarizes the characteristics of the Ir-192 source and the conditions for measuring the distance and angular dependence for each PSD.

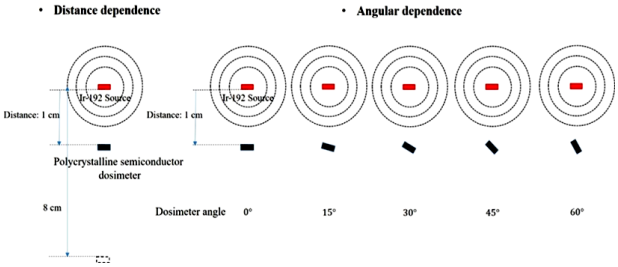

Figure 2. Measurement setups for distance dependence (left) and angular dependence (right) for two types of polycrystalline semiconductor dosimeters for the Ir-192 source.

Table 1. Characteristics of the Ir-192 source and measurement conditions for each polycrystalline semiconductor dosimeter for evaluating distance and angular dependence.

Ir-192 radioisotope source	
Radiation energy	Approximately 380 keV
Dose rate	4.69 Gy/min
Radiation dose	1 Gy/each measurement
Range of source to PSD surface distance	1–8 cm (Interval: 0.25 cm)
Irradiation angle	0–60° (Interval: 15°)

Ir-192: Iridium-192, PSD: polycrystalline semiconductor-based dosimeter

The distances of the PSDs from the Ir-192 source were determined based on dose measurements at 1 Gy for source-to-surface distances of 1-8 cm. The measurements were taken at 0.25-cm intervals from 1 to 3 cm and at 1-cm intervals from 3 to 8 cm. The signals measured by each PSD were normalized to the signal obtained at the reference distance of 1 cm.

The PSDs were positioned at a reference depth (1 cm below) from the Ir-192 source to evaluate their angular dependence, as shown in figure 2. The angular dependence was measured at angles of 0°, 15°, 30°, 45°, and 60° relative to the reference angle of 0°, where the central axis was parallel [11]. A dose of 1 Gy was delivered at all angles. The signals acquired at each angle were normalized to the signal acquired at the reference angle.

Monte Carlo simulation of distance and angular dependence

MC simulations were performed using the Geant4 Application for Tomographic Emission (GATE) v9.1 tool (OpenGATE Collaboration, CERN, Switzerland), which is widely used in medical imaging and radiotherapy research [12, 13]. The simulations replicated the experimental setup for evaluating the distance and angular dependence. Figure 3 shows a schematic diagram of the MC simulation used to evaluate the distance and angle dependence of the PSDs for the Ir-192 source. The Ir-192 source was modeled as a cylinder with a diameter of 0.035 cm and a length of 0.35 cm. The phase-space region had a length of 0.397 cm and a diameter of 0.045 cm. Table

[DOI: 10.61186/ijrr.24.2.3]

2 provides detailed information on the physical properties and dimensions of the source.

The dimensions of the PbI_2 and PbO materials were 1 × 1 × 0.015 cm, and they were positioned 1 cm from the cylindrical Ir-192 source. The number of particles was set to 1 × 108 to maintain statistical errors within 5% of the MC simulation. Table 3 provides detailed information on each material.

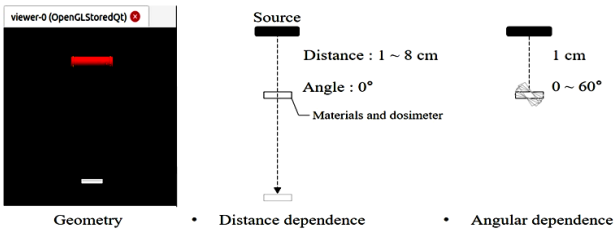

Figure 3. Schematic diagram of MC simulation for evaluating the distance and angle dependence of polycrystalline semiconductor dosimeters.

Table 2. Physical properties and size of Ir-192.

Physical properties			Size		
Atomic number	Mass number	Energy	Type	Diameter	Length
77	192	380 keV	Cylinder	0.35 mm	3.5 mm

Ir-192: Iridium-192.

Table 3. Physical properties of the PbI2 and PbO materials.

Material		Atomic number	Mass percent (%)	Molar mass (g/mol)	Density (g/cm^3)
PbI_2	Pb	82	44.9	461.1	6.16
	I	53	55.0		
PbO	Pb	82	92.8	223.2	9.53
	O	8	7.1		

I: Iodide; O: Oxide; Pb: Lead; PbI2: Lead (II) iodide; PbO: Lead (II) oxide.

Analysis of distance and angular dependence

The signal intensities from the MC simulations and measurements were analyzed using an inverse-square-law model, where the charge (Q) was a function of the distance (d), as expressed in equation (1).

$$Q = d^{-a} \quad (1)$$

The slope (-a) was compared with the theoretical value of -2 [14]. The coefficient of determination (R^2) was obtained from the trend line analysis. R^2 indicated how well the regression line (trend line) fitted the data; it ranges from 0 to 1, with values closer to 1 indicating a better fit. The distance (D_{50}) at which the signal intensity decreased by 50% was also determined in accordance with the recommendations of the International Commission on Radiological Units and Measurements [15]. The angular dependence was analyzed by normalizing the measured and simulated signals at each angle to the signal at the 0° reference angle.

Statistical analysis

The distance dependence was determined using SigmaPlot version 12.5 (Systat Software Inc., San Jose, USA). The experimental data were fitted to a power function, and the slopes of the fitted functions were subsequently compared to determine differences in distance dependence. This approach allowed for quantitative assessment of the relationship between distance and the measured response.

RESULTS

Distance dependence

Figure 4 shows the distance dependence of the normalization signal for the PSDs based on PbI_2 and PbO materials and the Ir-192 source.

Both experimental measurements (Meas.) and MC simulations (MCs.) are presented to demonstrate the variations in the signal with the distance from the Ir-192 source. The inverse square function curve (blue dotted line) was inserted, and the experimental and simulated data from both PSDs followed similar trends (figure 4).

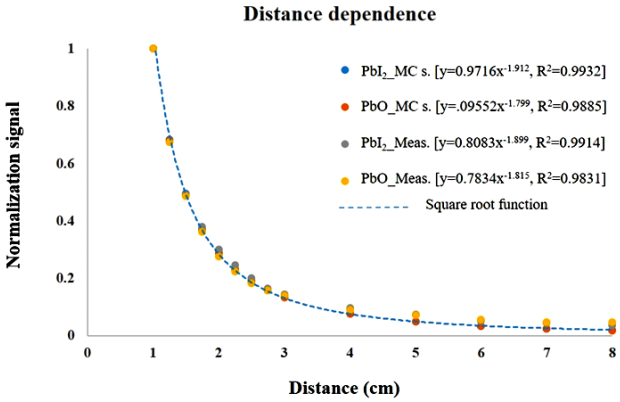

Figure 4. Normalized signal for experimental measurements (Meas.) and MC simulations (MC s) of polycrystalline semiconductor dosimeters fabricated from PbI2 and PbO materials as a function of distance relative to a distance of 1 cm from the Ir-192 source.

The slopes (-a) of the function based on the square root law for the PSD fabricated using PbI_2 material were -1.912 for measurements and -1.899 for MC simulations. The corresponding values for the PbO PSD were -1.799 and -1.815, respectively. The PbI_2 PSD had a slope closer to -2 than the PbO PSD, as confirmed by the measurements and MC simulations. The PbI_2 PSD had R^2 values of 0.9932 and 0.9914 for the measurements and MC simulations, respectively. The corresponding values for the PbO PSD were 0.9885 and 0.9831, respectively. The PbI_2 PSD had higher R^2 values for both the measurements and MC simulation results than the PbO PSD, although the difference was small (within 0.01). The D_{50} values for the PbI_2 PSD, representing the distance at which a 50% signal was detected, were 1.493 cm and 1.487 cm for the experimental measurements and MC simulation results, respectively. The D_{50} values for the PbO PSD were 1.488 and 1.481 cm, respectively. The D_{50} values for the two types of PSDs were almost identical for the experimental measurements and MC simulation results.

[DOI: 10.61186/ijrr.24.2.3]

Angular dependence

Figure 5 shows the angular dependence of the PbI_2 and PbO PSDs normalized at each angle and based on signals measured at 0° from an Ir-192 source.

The experimental measurements and MC simulation results demonstrated variation of the signal with the angle from the central axis of the Ir-192 source. The normalization signals from both PSDs decreased comparably with increasing PSD angle from 0 to 60° relative to the reference angle (0°) parallel to the Ir-192 source, as shown in figure 5. The acquired signals for the PbI_2 PSD decreased by approximately 21.6% and 20.4% for the experimental measurements and MC simulations, respectively, at an angle of 60° relative to that at 0°. The PbO PSD decreased by 24.6% and 24.5% for the measurements and MC simulations, respectively.

The maximum and minimum differences in the signals obtained from the measurements and MC simulations for the PbI_2 and PbO PSD were 4.56% and 1.28% at 15° and 0°, respectively. The maximum difference between the measurements and MC simulations for the PbO PSD was 5.48% at the dosimeter position angle of 60°. Differences of approximately 4% were observed at other angles. The differences were higher for the PbO PSD than for the PbI_2 PSD at all angles.

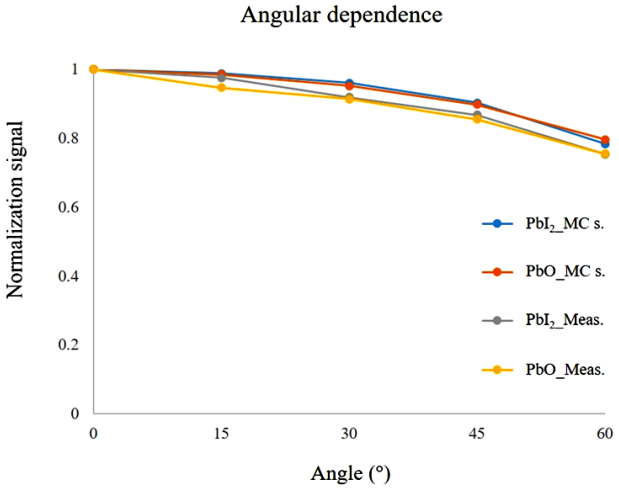

Figure 5. Normalized signal for experimental measurements (Meas.) and MC simulation (MC s) results of polycrystalline semiconductor dosimeters fabricated from PbI2 and PbO materials at angles relative to the reference angle (0°) from the Ir-192 source.

DISCUSSION

PbI_2 and PbO have been reported as promising photoconductor materials for the fabrication of PSDs. This is consistent with recent reports on the use of PSDs fabricated using them for radiation detection in the therapeutic energy range [16-18]. PbI_2 contains lead (Pb) and iodine (I), both of which have high atomic numbers (Z = 82 for Pb and 53 for I) that enable effective absorption of X-rays and gamma rays. Its relatively wide band gap contributes to its low noise characteristics and enhanced thermal stability [19]. Similarly, PbO (Z = 82) offers superior X-ray sensitivity to those of conventional materials such as silicon (Si) and cadmium zinc telluride. It is providing low dark current in photocurrent signals and is stable even under high-temperature conditions [20]. Emerging semiconductor materials such as cesium lead bromide perovskites and thallium bromide have also been actively investigated for medical dosimetry. They have demonstrated high sensitivity, but more comprehensive validation under brachytherapy conditions is warranted [21-23].

We fabricated PSDs using these two materials and investigated their distance and angular dependencies for the Ir-192 source, which is commonly used in brachytherapy. The experimental measurements were compared with the MC simulation results. Based on the findings, we investigated the applicability of these PSDs to quality assurance (QA) for brachytherapy with a high dose rate brachytherapy. However, research on the fabrication of PSDs using PbI_2 and PbO and evaluation of their distance and angle dependencies for Ir-192 radiation sources through measurements and MC simulations is limited. Dosimeters fabricated using polycrystalline thallium bromide and cesium lead bromide have been highlighted as QA tools for brachytherapy based on their performance with Ir-192 sources [23-25]. However, these studies only reported the measurement results and did not include any findings from MC simulations. Recent publications provide a broader context for interpreting the results of this study. MC-based approaches, such as GATE/Geant4 and RapidBrachyTG43, have been widely adopted to parameterize the TG-43 dose function and validate the anisotropy and radiation dose characteristics of Ir -192 sources [26, 27]. These studies highlight the need to combine experimental validation with MC modeling, which is consistent with the dual-approach methodology adopted in this study. Recent studies using small-volume ionization chambers and synthetic diamond detectors have reported angle-dependent discrepancies in results relative to those of MC simulations. These demonstrate that detector type and geometry significantly influence the angular response [28, 29]. They also support the findings of this study that angle correction factors are essential for accurate brachytherapy dosimetry.

The signals obtained based on the experimental and MC simulation results for the PBI_2 and PbO PSDs were confirmed to follow the inverse square law. They decreased sharply with increasing distance from the source for up to 8 cm (figure 3). The signal decay with distance was similar for the two PSDs based on the experimental measurements and simulation results. Both PSDs exhibited a power-law dependence with an exponent of approximately -2, which were

[DOI: 10.61186/ijrr.24.2.3]

consistent with the theoretical inverse-square-law behavior. This confirms their ability to accurately measure dose attenuation with distance. The high coefficients of determination ($R^2 > 0.98$) for all fits indicate strong agreement between the measured data and the power law model, validating the robustness of the model for characterizing distance dependence. The minor discrepancies between the Monte Carlo simulations and experimental measurements are attributed to geometrical factors, scattering effects, and material-specific interactions that are not fully accounted for in the simulations. The high R^2 values for all fits indicate strong correlations and suggest that a power-law model adequately represents the distance dependence of these semiconductor dosimeters. This study demonstrates the reliable and predictable distance dependence of the responses of the PbI_2 and PbO PSDs when they are exposed to Ir-192 sources.

The normalization signals from both PSDs, as determined from the measurements and MC simulations, decreased with increasing angle from 0° to 60°. The maximum decrease was approximately 25% at 60°. The Monte Carlo simulation and experimental measurement results for both dosimeters were in good agreement (<5%). The discrepancy of 5.48% for the PbO dosimeter at larger angles are within reasonable experimental error margins and do not significantly affect the overall angular dependence trend. The consistent angular dependence observed for the MC simulations and experimental measurements may highlight the reproducibility of the measurement setup for these dosimeters and the reliability of the data. However, the observed angular dependence of these two PSDs, especially the 25% decrease at 60°, highlights the need to implement an angular correction factor for clinical applications. Accurate angular correction is essential for improving dosimetry precision, especially for the complex treatment geometries encountered during brachytherapy. Future studies should explore real-time dose monitoring applications and optimize angular correction techniques to enhance clinical accuracy. Hybrid audit procedures and model-based dose calculation algorithms (MBDCAs) that integrate experimental dosimetry with MC-derived correction factors have received increasing attention in the clinical QA context [30, 31]. These developments align closely with our findings, especially the need for angular correction strategies. Establishing detector-specific correction algorithms or lookup tables for PbI_2- and PbO-based PSDs will be essential for robust clinical implementation.

The limitations of this study should be acknowledged despite the promising results. First, the measurements were performed under simplified conditions using a single ^{192}Ir source in a homogeneous environment Heterogeneous tissue, applicator geometry, and multi-source dwell positions may introduce additional uncertainties in clinical practice that were not captured in this study. Second, the angular dependence was evaluated only within the range of 0- 60°. However, more extreme geometrical configurations may occur during brachytherapy. Therefore, the findings of this study should not be extrapolated beyond the observed range. Third, the short-term reproducibility of the PbI_2- and PbO-based PSDs was verified. However, their long-term stability under repeated irradiation and varying environmental conditions such as temperature and humidity has not been established. Furthermore, the MC simulations employed simplified models of the source and phantom, which may have limited their ability to capture complex scattering phenomena and applicator-induced perturbations. Finally, this study confirmed the necessity of angular correction factors. However, a practical correction methodology for clinical implementation has not yet been established. Future research should focus on validating these dosimeters under clinically relevant geometries, assessing their long-term performance, and developing correction algorithms to facilitate their robust application in brachytherapy dosimetry.

CONCLUSION

PSDs were fabricated using PbI_2 and PbO, and their measurement performances, including distance and angle dependence, were evaluated for an Ir-192 source used for brachytherapy. The measured distance and angular dependence of the PSDs were in good agreement with the MC simulation results, which validated the fabrication process and measurement methodology. However, angular compensation is recommended for clinical applications because of the relatively high angular dependence of both PSDs at 60° from the Ir-192 source. Additionally, brachytherapy dosimetry and QA using PSDs should be performed with precise measurement setups to ensure accuracy.

***Acknowledgment*:** Not applicable.
***Conflict of interest*:** The authors declare no conflicts of interest.
***Funding*:** This work was supported by the National Research Foundation of Korea (NRF) grant funded by the Korea government (NRF-RS-2023-00212193) and by the Seoul National University Bundang Hospital (SNUBH) Research Fund (grant number 02-2023-0046).
***Ethical consideration*:** This study did not involve human participants or animals.
***AI usage statement*:** The authors declare that no generative AI tools were used in the preparation of this manuscript.

[DOI: 10.61186/ijrr.24.2.3]

***Conflicts of interest*:** The authors declare no conflicts of interest.

***Author's contribution*:** M.J.H and S.W.K: conceptualization, data collection, writing-original draft; K.Y.E, I.A.K, and J.S.K: data analysis; B.L and W.C: study administration; J.B.C: writing-review and editing, study supervision.

REFERENCES

1. Netkim A, Adenipekun A, Akinlade B, Campbell Q (2010) Evaluation of novel therapeutic approaches in oncology. *Clin Med Insights Oncol, **4**: 89*.
2. Watanabe Y, Maeyama T, Mizukami S, Tachibana H, Terazaki T, Takei H, *et al.* (2022) Analysis of radiation-induced DNA damage in human lymphocytes. *J Radiat Res, **63**(6): 838-45*.
3. Niroomand-Rad A, Backwell CR, Coursey BM, Gall KP, McLaughlin WL, Meigooni AS, *et al.* (1998) AAPM protocol for 3D dosimetry of radiation therapy. *Med Phys, **25**(10): 2093-115*.
4. Bechchar R, Senhou N, Ghassoun, J (2019) A fast and accurate analytical method for 2D dose distribution around brachytherapy sources in various thissue-equivalent phantoms. *Int J Radiat Res, **17**: 531-540*.
5. Kim KT, Heo YJ, Han MJ, Oh KM, Lee YK, Kim SW, *et al.* (2017) Development of a novel radiation detector using scintillating materials. *J Instrum, **12**(4): C04024*.
6. Rosenfeld AB, Biasi G, Petasecca M, Lerch MLF, Villani G, Feygelman V (2020) Advanced dosimetry techniques for modern radiation therapy. *Phys Med Biol, **65**(16): 16TR01*.
7. Rustgi SN (1998) Monte Carlo simulations in radiation therapy dosimetry. *Phys Med Biol, **43**(8): 2085-102*.
8. Acun H, Bozkurt A, Kemikler G (2017) Dosimetric investigation of high dose rate Ir-192 source with Monte Calro method. *Int J Radiat Res, **15**: 242-249*.
9. Mowlavi AA, Cupardo F, Severgnini M (2008) Monte Carlo and experimental relative dose determination for an Iridium-192 source in water phantom. *Iran J Radiat Res, **6**: 37-42*.
10. Briesmeister JF (2000) MCNPTM- A general Monte Carlo Nparticle transport code, Version 4C. Los Alamos National laboratory Report LA-13709-M, USA.
11. Hsu SM, Wu CH, Lee JH, Hsieh YJ, Yu CY, Liao YJ (2023) Investigation of apoptosis pathways in irradiated cancer cells. *PLoS One, **7**(9): e44528*.
12. Joya M, Nedaie HA, Geraily G, Rezaei H, Bromand A, Ghorbani M, *et al.* (2023) Assessment of radiation dose distribution in brachytherapy. *J Med Phys, **48**(4): 268-75*.
13. Oh G, Lee J, Kim H, Kim W, Kang S, Chung J, *et al.* (2024) Physiological responses to low-dose radiation exposure. *Front Physiol, **15**:1302301*.
14. Han MJ, Kang SW, Cho W, Kim JS, Kim IA, Chung JB (2024) Evaluation of photoconductor and scintillator hybrid dosimeters for radiation therapy quality assurance. *J Instrum, **19**(9): P09035*.
15. International Commission on Radiation Units and Measurements (2013) Prescribing, recording, and reporting photon-beam intensity-modulated radiation therapy (IMRT). *J ICRU, **13**(1): 1-73*.
16. Bennett PR, Shah KS, Dmitriev Y, Klugerman M, Gupta T, Squillante M, *et al.* (2003) Development of high-resolution gamma-ray detectors for medical imaging. *Nucl Instrum Methods Phys Res A, **505**(1-2): 269-72*.
17. Semeniuk O, Grynko O, Decrescenzo G, Juska G, Wang K, Reznik A (2017) Investigation of photoconductive properties of novel semiconductor materials. *Sci Rep, **7**(1): 8659*.
18. Han MJ, Yang SW, Bae SI, Moon YM, Jeon W, Choi CW, *et al.* (2021) Evaluation of a new dosimetric system for radiation therapy applications. *PLoS One, **16**(5): e0251441*.
19. Cho G (2008) Advances in nuclear medicine imaging techniques. *Nucl Med Mol Imaging, **42**(2): 88-95*.
20. Pineau E, Grynko O, Thibault T, Alexandrov A, Csik A, Kokenyesi S, *et al.* (2022) Development of novel sensors for radiation detection. *Sensors (Basel), **22**(16): 5998*.
21. Talamonti C, Kanxheri K, Pallotta S, Servoli L (2021) Diamond Detectors for Radiotherapy X-Ray Small Beam Dosimetry. *Front Phys, **9**: 632299*.
22. Granero D, Perez-Calatayud J, Ballester F (2005) Monte Carlo calculation of the TG-43 dosimetric parameters of a new BEBIG Ir-192 HDR source. *Radiother Oncol, **76**(1): 79-85*.
23. Yang SW, Han MJ, Shin YH, Jung JH, Cho HL, Park SK (2023) Development of quality assurance dosimeter for brachytherapy based on CsPbBr3 and evaluation of applicability. *J Instrum, **18**(6): P06024*.
24. Han MJ, Yang SW, Jung JH, Lee DH, Kim JY, Cho SJ, *et al.* (2022) Performance analysis of a new radiation detector for medical applications. *J Instrum, **17**(2): P02010*.
25. Yang SW, Park SK, Moon CW, Kim KH (2023) Design and characterization of a compact dosimeter for radiation therapy. *J Instrum, **18**(7): P07021*.
26. Kalinowski J, Enger SA (2024) RapidBrachyTG43: A Geant4-based TG-43 parameter and dose calculation module for brachytherapy dosimetry, *Med Phys, **51**(5): 3746-3757*.
27. Wu J, Xie Y, Ding Z, Li F, Wang L (2021) Monte Carlo study of TG-43 dosimetry parameters of GammaMed Plus high dose rate 192Ir brachytherapy source using TOPAS. *J Appl Clin Med Phys, **22**(6): 146-153*.
28. Feldman J and Orion I (2016) Small volume ionization chambers angular dependence and its influence on point-dose measurements. *Int J Med Phys Clin Eng Radiat Oncol, **5**(1): 26-32*.
29. Angelou C, Patallo IS, Doherty D, Romano F, Schettion G (2024) A review of diamond dosimeters in advanced radiotherapy techniques, *Med Phys, **51**(12):9230-9249.*
30. Pappas EP, Zoros E, Moutsatsos A, Peppa V, Zourari K, Karaiskos P, Papagiannis P (2017) On the experimental validation of model-based dose calculation algorithms for 192Ir HDR brachytherapy treatment planning, *Phys Med Biol, **62**(10): 4160-4182*.
31. Sloboda RS, Morrison H, Cawston-Grant B, Menon GV (2017) A brief look at model-based dose calculation principles, practicalities, and promise. *J Comtemp Brachytherpay, **9**(1): 79-88*.

[DOI: 10.61186/ijrr.24.2.3]